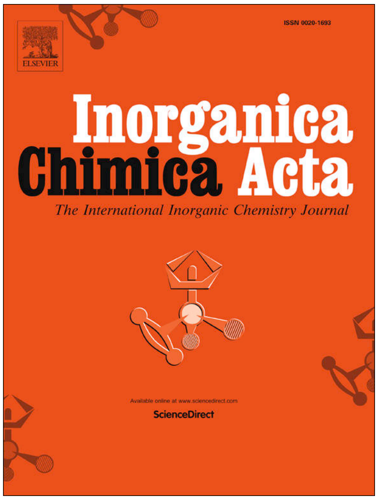

Research paper

Transesterification Activity by a Zinc(II)-Schiff Base Complex with Theoretical Interpretation

Chanchal Kumar Pal, Shreya Mahato, Mayank Joshi, Suvendu Paul,
Angshuman Roy Choudhury, Bhaskar Biswas

PII: S0020-1693(20)30077-3
DOI: https://doi.org/10.1016/j.ica.2020.119541
Reference: ICA 119541

To appear in: *Inorganica Chimica Acta*

Received Date: 14 January 2020
Revised Date: 18 February 2020
Accepted Date: 18 February 2020

Please cite this article as: C. Kumar Pal, S. Mahato, M. Joshi, S. Paul, A. Roy Choudhury, B. Biswas, Transesterification Activity by a Zinc(II)-Schiff Base Complex with Theoretical Interpretation, *Inorganica Chimica Acta* (2020), doi: https://doi.org/10.1016/j.ica.2020.119541

Transesterification Activity by a Zinc(II)-Schiff Base Complex with Theoretical Interpretation

Chanchal Kumar Pal,[a] Shreya Mahato,[a] Mayank Joshi,[b] Suvendu Paul,[c] Angshuman Roy Choudhury, [b] Bhaskar Biswas[a,*]

[a]*Department of Chemistry, University of North Bengal, Darjeeling-734013, India*
[b]*Department of Chemical Sciences, Indian Institute of Science Education and Research, Mohali, Sector 81, Knowledge City, S. A. S. Nagar, Manauli PO, Mohali, Punjab 140306, India*
[c]*Department of Chemistry, University of Kalyani, Kalyani 741235, West Bengal, India*

Abstract

The article demonstrates the synthesis, structural characterization and transesterification activity of a mononuclear zinc(II) complex, $[Zn(H\mathbf{L})(H_2O)].(H_2O)$ (**1**) containing a previously reported Schiff base ligand, $H_3\mathbf{L}$ = *N,N′*-bis(salicylidene)-1,3-diamino-2-propanol]. X-ray structural analysis of **1** reveals that Zn(II)-Schiff base complex crystallizes in hexagonal crystal system with $P6_1$ space group and adopts a distorted tetrapyramidal geometry. Self-assembled molecular units of **1** exhibit a beautiful construction of 3D crystalline architecture through intermolecular hydrogen bond wire. Zinc(II) complex displays an enhancement of fluorescence intensity in comparison to H**L** in methanol medium. Catalytic behaviour of **1** towards disodium salt of 2,4-dinitrophenylphosphate (PNPP) in aqueous-methanol medium exhibits good transesterification activity with initial rate constant value of 1.73×10^{-4} min^{-1}. Detailed DFT calculations are also employed to cope with the geometrical parameters of **1** as well as to explore the proposed catalytic mechanism of transesterification activity.

Keywords: DFT Study; Schiff Base; Transesterification Activity; X-ray Structure; Zinc(II)

*Corresponding author. E-mail: bhaskarbiswas@nbu.ac.in / icbbiswas@gmail.com

1. Introduction

Now-a-days, coordination compounds of 3d metal ions have created huge appeal for their impeccable contributions and key functions in the chemistry of metallo-enzymes and biology [1-5]. Paramount attentions have further been focused on to develop advance functional materials by tuning electronic and steric factors of ligands mediated through different types of metal ions [6-16]. Among the transition metal ions, for the easy availability and cost effectiveness, 3d metal complexes are highly dominant in nature and material science. Zinc, one of the most significant bio-metals in nature exhibit promising opto-electronic, luminescent, biological and catalytic properties and one of the potential candidates in bringing novelty in the arena of advance materials [17-27].

Nature is the utmost source in scientific research which reveals invaluable impact of coordination compounds in metal dependent bio-catalysis. Thus, considerable attentions have been devoted in bioinorganic chemistry aiming to study on zinc complexes mediated bio-inspired catalytic systems those are able to emphasize the active sites of metallo-enzymes.[26,27] Zinc(II) based coordination compounds play significant role in living world those are potentially considered as photo-active materials.[24,25] Important physico-chemical properties including Lewis acidic behaviour, nucleophile generation, swift ligand exchange, and stabilization of leaving group present Zn(II) ion one of the most ubiquitous candidate in biology.[17,27] In the wide range of metallo-enzymes, phosphoesterase enzymes have great exposures in bio-remediation of organophosphate compounds, DNA fragmentation, RNA replication, bone metabolism, and chemotherapy [28]. Metal ions are coordinated through N atom of histidine ligands, O-atom of aspartate, and often including a metal ion-bridging hydroxide ion in the active site of the phosphoesterase [29].

Literature survey revealed that S. Uhlenbrock *et al.* [30a] produced a trinuclear zinc(II) complex using the same Schiff base and this same Schiff base is used by R. Bagai *et al.* [30b] to prepare a tetranuclear manganese complex while P.E. Kruger *et al*. [30c] synthesized a dinuclear copper(II) complex by utilizing this same ligand. Eventually, we also prepared a trinuclear Zn(II) complex, a dinuclear Fe(III) complex, a mononuclear Cu(II) complex using this same Schiff base ligand [31]. Moreover, coordination behavior of the ligand has been further tested towards Zn(II) ion by addition of methoxo groups to the ligand backbone of this Schiff base [32]. In this present endeavour, we report the synthesis, spectroscopic characterization, X-ray structure and fluorescence behaviour of a new Zn(II)-Schiff base complex. This Zn(II) complex exhibits potential transesterification activity towards disodium salt of 2,4-dinitrophenylphosphate (PNPP) and rate of transesterification activity was found as

1.73×10^{-4} min^{-1}. Experimental and computational observations recommend that Zn(II)-bound aqua molecule produces effective nucleophile in solution in the course of bio-catalysis and proceeds through organophosphorous intermediate in solution.

2. Experimental Section

2.1. Preparation of the zinc(II)-Schiff base complex

(a) Chemicals, solvents and starting materials

High purity salisaldehyde (E-Merck, India), 1,3-diaminopropan-2-ol (Alfa-Aesar, UK), zinc(II) chloride hexahydrate (E- Merck, India) and disodium salt of p-nitrophenylphosphate (SRL, India) were purchased from respective concerns and used as received. All the other reagents and solvents of analytical grade were purchased from repute commercial sources and used without further purification.

(b) *Synthesis of the Schiff base and zinc(II) complex*

The synthetic procedure of the Schiff base complex was described in details elsewhere [30,31]. Salisaldehyde (0.245 g, 2 mmol) was treated with 1,3-diaminopropan-2-ol (0.090 g, 1 mmol) in 25 mL ethanol under refluxing condition. After 8h, the reaction solution was evaporated to yield a yellow solid compound, which was dried and stored over $CaCl_2$ for use. Yield, 0.270 g (90.6%). Anal cal. for $C_{17}H_{18}N_2O_3$ ($H_3\mathbf{L}$): C, 68.44; H, 6.08; N, 9.39; Found: C, 68.48; H, 6.01; N, 9.33. ^1H NMR ($CDCl_3$) $\delta = 3.68$ (dd, $J = 12.4, 6.8$ Hz, 2H), 3.84 (dd, $J = 12.4, 4.0$ Hz, 2H), 4.23-4.25 (m, 1H), 6.88 (t, $J = 7.2$ Hz, 2H), 6.96 (d, $J = 8.4$ Hz, 2H), 7.25 (dd, $J = 7.6, 1.6$ Hz, 2H), 7.32 (td, $J = 8.8, 1.6$ Hz, 2H), 8.41 (s, 2H) ppm. ^{13}C NMR δ, 62.9, 70.2, 117.0, 118.5, 118.6, 131.5, 132.5, 161.1, 167.3 ppm. IR (KBr, cm^{-1}): 1634, 1602 ($\nu_{C=N}$), 3409 (ν_{OH}); UV-Vis (λ_{max}, nm, 10^{-4} M, MeOH): ~254, 313, 404.

~10 ml methanolic solution of $ZnCl_2.6H_2O$ (0.255 g, 1.0 mmol) was added to 15 ml solution of $H_3\mathbf{L}$ (0.300 g, 1.0 mmol) in the same solvent (15 ml). The pale yellow Schiff base solution was turned to bright yellow and slow evaporation of the reaction mixture produced pale yellow coloured crystalline compound after 8-10 days. Yield: 0.171 g (67.0 % based on metal salt). Anal. Calc. for $C_{17}H_{20}N_2O_5Zn$ (**1**): C, 51.34; H, 5.07; N, 7.04. Found: C, 51.37; H, 5.01; N, 7.09 %. IR (KBr, cm^{-1}): 3471 (ν_{OH}), 1618 ($\nu_{C=N}$), 1257 (ν_{PhO}); UV-Vis (λ_{max}, nm, 10^{-4} M, MeOH): 244, 297, 337.

2.2. Physical measurements

FTIR-8400S SHIMADZU spectrometer (Shimadzu, Kyoto, Japan) was employed to record IR spectrum (KBr) of **1** in the range of 400-3600 cm^{-1}. ^{1}H NMR spectrum of ligand was obtained in $CDCl_3$ on a Bruker Avance 300 MHz spectrometer (Bruker, Massachusetts, USA) at 298 K and was recorded at 299.948 MHz. Steady-state absorption spectral measurements were performed with a JASCO model V-730 UV-Vis spectrophotometer (Jasco, Tokyo, Japan). Elemental analyses were performed on a Perkin Elmer 2400 CHN microanalyser (Perkin Elmer, Waltham, USA). Electrospray ionization (ESI) mass spectra of **1** and the reaction mixture of **1** in presence of pNPP were recorded on a Q-TOF MicroTM Mass Spectrometer (Waters Corporation, Massachusetts, USA). Steady-state fluorescence spectral measurements were performed with a Hitachi F-7000 spectrofluorimeter (Hitachi, Tokyo, Japan). Molar conductivity measurement was performed using a LAQUA Benchtop DS70 conductivity meter (Horiba, California, USA). The pH values of the solutions were measured using a Labman pH meter (Wensar, Chennai, India) at 298 K.

2.3. X-ray diffraction analysis

X-ray single crystal diffraction data for **1** was collected using a Rigaku XtaLABmini diffractometer equipped with Mercury CCD detector. The data were collected with graphite monochromated Mo-Kα radiation (λ=0.71073 Å) at 100.0(2) K using ω scans. The data were reduced using CrysAlisPro 1.171.39.7f [33] and the space group determination was done using Olex^2. The structure was resolved by dual space method and refined by full-matrix least-squares procedures using SHELXL-2015 software package through OLEX^2 suite [34,35]. The oxygen atom (O4) was found disordered over Axial and equatorial positions. To treat that appropriately, the adjoining C atoms were splitted and refined as two fractions.

2.4 Hirshfeld surface analysis

Hirshfeld surfaces and fingerprint plots were generated using Crystal Explorer 17.5 [36] using data of single crystal X-ray diffraction study. The function d_{norm} is a ratio of the distances of any surface point to the nearest interior (d_i) and exterior (d_e) atom and the van der Waals radii of the atoms [37,38]. The negative value of d_{norm} indicates the sum of d_i and d_e is shorter than the sum of the relevant van der Waals radii, which is considered to be a closest contact and is visualized in red colour. The white colour denotes intermolecular distances close to van der Waals contacts with d_{norm} equal to zero whereas contacts longer than the sum of van der Waals radii with positive d_{norm} values are coloured with blue. A plot of di versus de is a fingerprint plot which identifies the presence of different types of intermolecular interactions.

2.5. Transesterification activity of Zn(II)-Schiff base complex (**1**)

PNPP was employed as a standard substrate to examine transesterification activity in aqueous-methanolic medium following a reported procedure [39,40]. An initial screening of the hydrolytic tendency of the Zn(II)-Schiff base complex was performed until 2% formation of 4-nitrophenolate was reached, and then its kinetic data were collected. The hydrolysis rate of PNPP in the presence of the Zn(II) complex was measured by an initial rate method, keeping the incremental absorbance of the electronic band fixed at 418 nm for releasing of 4-nitrophenolate ion in aqueous-methanolic mixed solution at 298 K. For the wavelength scan, the spectra were recorded by addition of 1×10^{-4} (M) Zn(II) complex solution to 1×10^{-3} (M) PNPP solution for ~1 hour. Blank experiment with PNPP in absence of Zn(II) complex under identical reaction conditions were performed and did not show any phosphatase activity.

Kinetic experiments for the phosphoester cleavage study were carried out by monitoring the growth of the 4-nitrphenolate species at 418 nm as a function of time under the condition of excess substrate in presence of Zn(II) complex, keeping the other parameters constant. Kinetic experiment was performed with 1×10^{-4} (M) concentration of Zn(II)-Schiff base complex and PNPP {varying the concentration from 1×10^{-3} to 1×10^{-2} (M)} in H_2O-CH_3OH mixed solvent adopting UV-Vis spectrophotometer. The spectrophotometric titration was carried out for a total period of 70 mins with 06 minutes interval. All measurements were performed in triplicate and arithmetic average was reported.

2.6. Computational details

Avoiding all types of symmetrical constraints, all quantum chemical computations were executed with Gaussian 09W program suite [41] and GaussView 5.0 was exercised to extract graphical figures as well as to view Gaussian input and output files [41]. For ground and excited singlet state computational calculations, density functional theory (DFT) and Time Dependent Density Functional Theory (TD-DFT) were respectively considered. For computational calculations, B3LYP theoretical model and 6-311G basis set [42] were employed for both the metal and non-metallic elements. Initially, the Zn(II)-complex was optimized in vacuum and global minima was confirmed through IR frequency calculation and stability check-up. Then, optimized structures in vacuum were again optimized in methanol (MeOH, ε=32.613) following Integral Equation Formalism Polarisable Continuum Model (IEFPCM) [43] to include solvent effect and corroborate with the experimental results. For further details of computational specifications, readers could follow somewhere else [44].

3. Results and discussion

3.1. Synthesis and formulation of the Zn(II)-Schiff base complex (**1**)

The Zn(II)-Schiff base complex was prepared in single crystals by mixing of Zn(II) chloride with an (N,O)-donor Schiff base ligand in 1:1 mole ratio in an aqueous methanolic medium (Scheme1). Variation of Zn(II) salts in this reaction might lead to different Zn(II)-Schiff base complexes. It was already observed and reported that Zn(II) acetate salt in reaction with this Schiff base produced an acetate-bridged trizinc(II)-Schiff base complex [31]. The structural composition of **1** was determined by different spectroscopic and analytical techniques like IR, UV-Vis, ^{1}H NMR, ESI-Ms, molar conductivity including single crystal X-ray diffraction study.

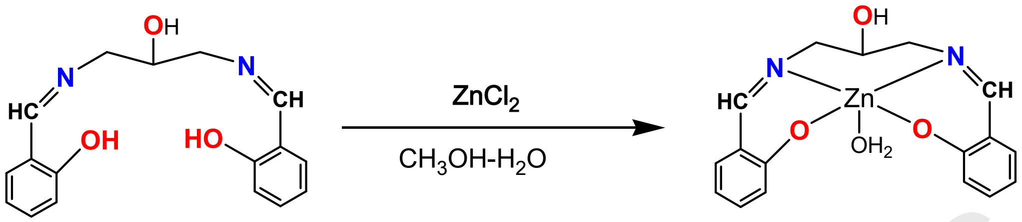

Scheme 1. Synthetic route of the Zn(II)-Schiff complex (**1**).

3.2. Description of crystal structure and optimized molecular structure

The coordination geometry of this Zn(II)-Schiff base complex is determined by X-ray structural analysis which reveals that Zn(II) complex crystallizes in hexagonal crystal system with $P6_1$ space group. An ellipsoidal plot of the crystal structure of **1** is shown as Figure 1. The structural refinement parameters are tabulated in Table 1. Selected bond angles and bond distances of **1** are listed in Table 2. The Zn(II) centre exists in a distorted tetrapyramidal geometry in crystalline phase as Zn(II) centre is out of plane which created by O1O2N1N2 atoms of ligand backbone. The average Zn-N bond distance values are longer than average Zn-O bond distance values (Zn1-N$_{av}$ = 2.116 Å; Zn1-O$_{av}$ = 2.021Å) in the pyramidal base. The apical bond distance is found shortest (1.983 Å) among all the metal-ligand donor coordination in the Zn(II) complex. Literature survey suggests that this ligand can exhibit a diversified mode of coordination based on the nature of metal ions. In general, this Schiff base may be considered as a pentadentate chelating ligand although during the formation of metal chelates, H$_3$**L** acts as a tetradentate chelator towards Cu(II) and Zn(II) ions, and exhibits its pentadentate behaviour towards Fe(III) ions.[31] Isolation of single crystals for monocopper(II) complex, diiron(III) complex and a trinuclearzinc(II) complex employing this ligand strongly account on this fact.[31] Moreover, H$_3$**L** is utilized to develop d-block metallo-clusters in crystallize phase with greater magnetic importance [30]. In real sense, H$_3$**L** is an example of flexidentate ligand in coordination chemistry. To examine the nature of weak forces in self-assembled crystalline architecture for this Zn(II)-Schiff base complex, it is observed that phenolate oxygens (O1,O2) and coordinated O(O3) in aqua molecule act as donors while H atoms attached to aromatic-C (C10A) and coordinated aqua molecule (H3A, H3B) behave as accepter in the construction of 3D crystalline architecture through strong to moderate H-bonding interactions [Fig. S1; O3-H3A…O1, 2.21 Å, O3-H3B…O1, 1.93Å, C10-H10A…O2, 2.57 Å].

Previously, we reported the preparation and crystal structure of an isostructural Zn(II)-Schiff base complex, [Zn(H**L**^{1})(H_2O)] (where H_3**L**^{1} = *N,N′*-bis(3-methoxysalicylidene)-1,3-diamino-2-propanol) using o-vanilin instead of salicyldehyde [20]. Interestingly, adding of methoxy substituent to the ligand skeletal didn't effect a much and displays almost identical mode of coordination towards Zn(II) ion. A comparison of structural aspects between X-ray structures of [Zn(H**L**)(H_2O)] and [Zn(H**L**^{1})(H_2O)] (Table S1) clearly present the tetradentate chelating mode of coordination for both the Schiff base ligands [20]. From crystallographic perspectives crystal system and space group are entirely different. Solvents of crystallization is found for [Zn(H**L**)(H_2O)] structure (Table S1).

Structural correlation between the DFT optimized structure and X-ray structure arecopmpared in Table Table 2 employing DFT study. Also, the optimized molecular structure of Zn(II)-Schiff base complex in vacuum (Fig. 2) resembles well with crystal structure. Computationally calculated bond length and bond angle values are in well agreement with the crystallographic bond distance and bond angle values (Table 2). The mode of coordination for ligand to metal centre exhibits close similarities between the coordination geometry of theoretical and XRD structure. A superimposition of the XRD structure with optimized structure is also performed using PyMOL 1.3 software and presented in Fig. S2. This atom to atom superimposition between the XRD and optimized structure of **1** validates the computational results more profoundly.

3.3 Hirshfeld surface analysis

The hirshfeld surface of Zn(II) complex is shown in Figure S3 and display surface is plotted with d_{norm}. The hirshfeld surface is unique for given crystal structure which proposes the opportunity of locating additional understanding to the crystal. The quantitative measures like volume (507.83 Å^3), area (451.69 Å^2), globularity (0.681) and asphericity (0.368) also computed using hirshfeld surface. In this molecule hydrogen bonding between

oxygen and hydrogen atoms which is seen in red spots on the hirshfeld surface (Fig. S3). Percentage share of each element in close interaction (Table S2) and fingerprint plots (Fig. 3) are showing the area of intense interaction with other molecule. In the fingerprint plot also, the direction of interaction is displayed towards O of bridging molecule from oxygen of water molecule as seen in red region of hirshfeld surface.

3.4. Experimental observations on solution properties of Zn(II) complex and calculated frontier orbitals

The zinc(II) compound is soluble in common polar solvents like methanol, acetonitrile and water. The electronic spectrum of Schiff base in methanolic solution consists of high intensity electronic transitions at 254 and 313 nm which are assignable to π→π* and n→π* transitions correspond to –C=N- chromophore of Schiff base ligand (Fig. S4).[20,31] The optical spectrum for the Zn(II)-Schiff base complex in methanol medium exhibits electronic transitions at 244, 297 and 337 nm (Fig. S4). Electronic transitions correspond to 244 and 297 nm are assignable to π→π*/n→π* transitions while the electronic band at 337 nm represents the intra-ligand charge transfer in the Zn(II)-Schiff complex. The electronic bands for zinc(II) complex remains almost unaffected after keeping the solution for 3 days in MeOH at RT. This observations account on the structural rigidity for **1**.

TD-DFT is employed to cope the electronic properties of Zn(II) complex in excited states. To gain the insights of the nature of optical spectrum of Zn(II) complex, TD-DFT studies are performed. The low energetic electronic transitions in HOMO→LUMO/ HOMO-1→LUMO+1 and HOMO-2→LUMO+2 (Fig. 4) portray a deep view of the level of chemical reactivity for this Zn(II) complex in MeOH. The electronic cloud of HOMO, HOMO-1 and HOMO-2 are majorly located on the ligand moiety and on contrary, the electronic cloud of LUMO, LUMO+1 and LUMO+2 are redistributed throughout the ligand moiety avoiding the Zn(II) portion. Also, there occurs a reorientation of electron cloud within the ligand moiety on transition from filled to unfilled FMOs. This indicates the possibility of intra ligand charge transfer (ILCT) phenomenon [45]. Therefore, from computational calculation, it may be supported the possibility of ILCT. Also, the HOMO-LUMO, HOMO-1 to LUMO+1 transition energies 3.92 eV (316 nm), 4.19 eV (296 nm) are very close to absorption spectra of the Zn(II) complex. Thus, it may be recommended that electronic transitions among these FMOs are majorly contributed for UV-Vis spectrum of the Zn(II) complex.

Molar conductivity of the Zn(II) complex is recorded at 298 K. A solution of 1.240×10^{-3} (M) concentration produces molar conductance as 6.1 µS/m. Molar conductivity data for this Zn(II) complex recommends about the non-electrolytic nature and solution phase stability for the Zn(II)-Schiff base complex.

The luminescence spectrum of the Zn(II) compound (λ_{ex}, 244, 297 nm) in methanol (Fig. S5) portrays the emission behaviour of the Zn(II)-Schiff base complex. The emission wavelength is found to be at ~ 357 nm (Fig. S5). It is observed that the fluorescence intensity enhances by more than 2 fold in comparison to the fluorescence intensity of the Schiff base. Incorporation of Zn(II) ion ($3d^{10}$ system) in Schiff base may bring structural rigidity in solution phase and this phenomenon accounts in favour of enhancement of fluorescence intensity over the ligand [10b,18,20].

3.6. Transesterification study of Zn(II)-Schiff base complex

A 10^{-4} M aq. methanolic solution of zinc(II)-Schiff base complex is added to the solution of 10^{-3} (M) PNPP and a new electronic band with incremental absorbance at 418 nm is started to develop (Fig. 5). This new electronic band at λ_{max}, 418 nm may be attributed to the growth of 4-nitrophenolate ion in solution in this course of transesterification activity [6b,8b,22,39]. The observed spectral changes are displayed in Fig. 5.

The kinetic parameters related to transesterification study are determined following initial slope method. The initial rate constant, V(min^{-1}) is found as 1.73×10^{-4} (Error = 8.37×10^{-5}) which is determined from the plot of $\log[A_\alpha/(A_\alpha - A_t)]$ versus time (Fig. 6) in this catalytic transesterification study [6b,8b,22,39]. The nature of plot seems to be a first order kinetics and maintains a good linearity with $R^2 = 0.978$. Control experiments are also performed to examine the non-catalytic role of Schiff base, and the experiments under similar reaction conditions are found non-responsive towards transesterification activity of PNPP. A literature survey on the rate of catalytic transesterification study of zinc(II) complexes is made to compare the level of activity of this zinc(II) with reported compounds (Table 3) [46-52].

Previous scientific investigations made by renowned scientists and their group provide some source of lights in proposing the mechanistic pathway for the course of transesterification study. In general, Lewis acid activation, leaving group activation and metal-nucleophile attack to substrate remain the catalytic route of transesterification activity for the enzymes (Scheme 2) [6b,8b,22,39, 46-54].

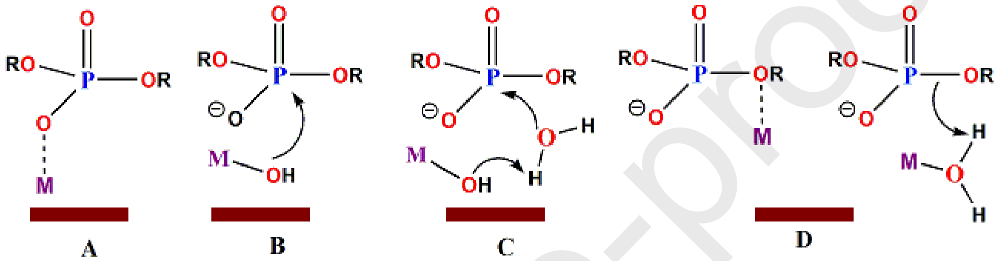

Scheme 2. Modes of activation for metal catalysed transesterification activity towards phosphoester substrates

ESI-Ms of this Zn(II) complex in presence of PNPP is recorded and the rise of important peaks with isotopic distribution pattern is noted. The spectrum (Fig. S6) displays an important peak at m/z 596.6761 (cald. 596.8680) which is attributed to the existence of substrate-enzyme adduct in solution phase. Another important peak at m/z 459.8944 in the mass spectrum is indicative of the presence of organophosphorous intermediate species and peak at 161.1078 m/z is evident for the development of by phenolate species (calcd. m/z 161.09) in solution. The presence of such peaks in ESI-Ms provides sufficient light about the nucleophilic attack by aqua molecules to P atom of PNPP which actually facilitates hydrolytic cleavage of PNPP. Zn(II) ions always behave as a good Lewis acid and this property facilitates the generation of Zn(II)-OH nucleophile. In this regard, pK_a value of the coordinated aqua molecule is calculated which strongly suggests the nucleophilic behavior towards PNPP. This phenomenon represents the formation of organophosphorus intermediate by nucleophilic attack to PNPP, and consequently, 4-nitrophenolate ion evolutes in solution. Finally, it decomposes to the active form of Zn(II)-Schiff base complex.

Based on information obtained from literatures and spectroscopic as well as analytical observations, the proposed mechanistic cycles may be presented as follows. (Scheme 3) [6b,8b,22,39,46-54].

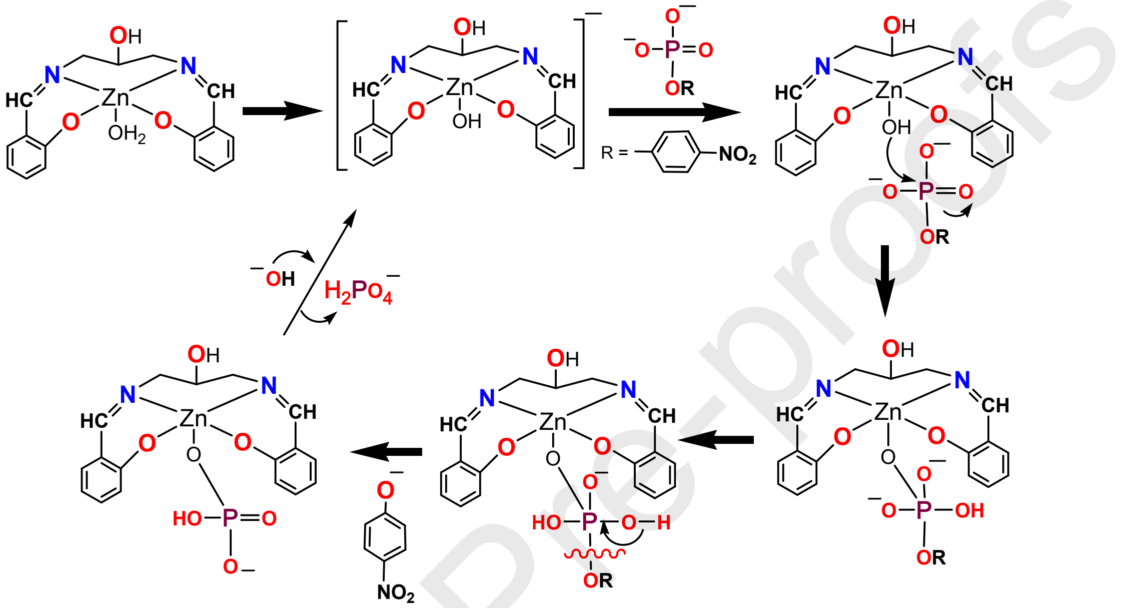

Scheme 3. Plausible catalytic cycle for phosphoester cleavage study by Zn(II)-Schiff base

Recently, different scientific groups focused on exploration of mechanistic aspect of the phosphoestarese activity of dinuclear Zn(II) complexes theoretically employing density functional theory [54-57]. However, an effort is made to explore the plausible catalytic pathways of transesterification study by this mononuclear zinc(II)-Schiff base complex based on systematic DFT study.

To rationalize the catalytic pathway of Zn(II) complex DFT study is carried out to perform detailed computational calculations. All the intermediates (I-V, Scheme 4) of the catalytic process are optimized in methanol and the Cartesian coordinate values of the intermediates are presented in Tables S3-S7 (ESI) respectively. Detailed exploration of literature of catalysis mechanisms alongwith spectroscopic as well as analytical observations enforced us to propose the above mentioned mechanistic pathway (Scheme 2) [6b,8b,22,39,46-53]. Hence, from optimized geometries, calculations are made to determine the binding energies of the intermediates aiming to establish their thermodynamic criteria of formation within the cyclic pathway. Initially, the Zn(II) complex (I) loses a proton and converted into the active form of Zn(II)-Schiff base complex (II). Then, the active form (II) initiates nucleophilic attack to PNPP and generates the intermediate III which converted into IV. The Intermediate (IV) releases 4-nitrophenolate ion in solution and converted in (V). Finally, the intermediate (V) regenerates the active form of the catalyst (II) to initiate the cycle again and again.

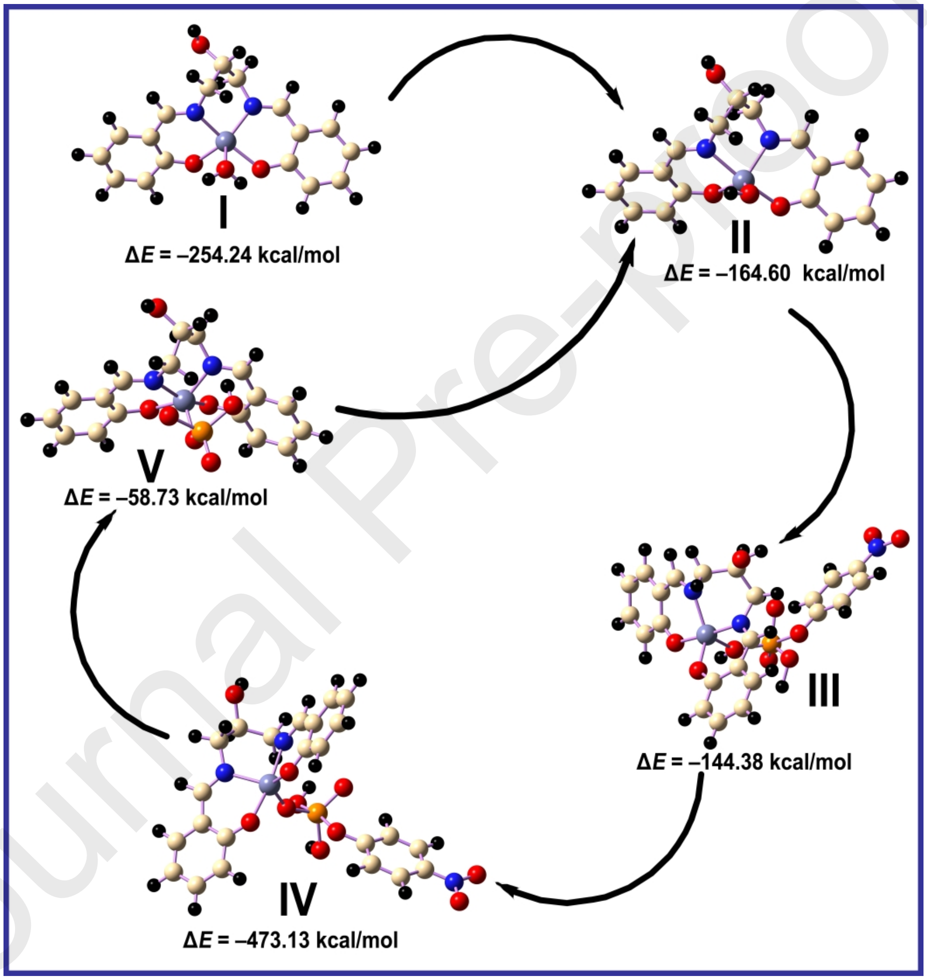

Scheme 3. DFT optimized structures of the intermediates of plausible mechanistic cycle of catalytic activity of the Zn(II) complex along with interaction energy values.

Most incredibly, the binding energies of all the intermediates are found to be negative that allowed the thermodynamic criteria of formation of the mentioned intermediates. Therefore, it can be stated that the above mentioned mechanism (Scheme 3) must be the plausible mechanism of the transesterification activity of the Zn(II) complex.

4. Conclusion

In summary, we synthesize a Zn(II)-Schiff base complex with a flexidentate chelator and determined its square pyramidal coordination geometry with single crystal X-ray analysis including different spectroscopic and analytical techniques. DFT computations recommend about intra-ligand charge transfer properties of **1** in solution phase. The complex shows good photo-luminescence property in methanolic solution. This Zn(II)-Schiff base complex displays good transestrification reaction of PNPP in aq. methanolic medium with initial rate constant, V(min^{-1}) = 1.73×10^{-4}. The computational calculations interpret the experimental observations very well. Synthesis of bio-inspired Zn(II)-Schiff base complexes as catalysts aren't highly abundant in literatures and investigation of bio-mimicking property of this Zn(II) complex may provide valuable information about biological process. Good luminescent properties of this Zn(II)-Schiff base complex may bring advancement in designing opto-electronic devices. Moreover, this mononuclear Zn(II) complex can be employed as a metallo-ligand to develop multidimensional structural aspects in Zn(II) based coordination compounds.

5. Supplementary data

Crystallographic data are available free of charge from The Director, CCDC, 12 Union Road, Cambridge, CB2 1EZ, UK (fax: +44-1223-336033; E-mail: deposit@ccdc.cam.ac.uk or www: http://www.ccdc.cam.ac.uk) upon request, quoting deposition number CCDC 1900186 for the Zn(II) complex.

Acknowledgement

BB thanks Science and Engineering Research Board (SERB) for financial support under the Teacher Associateship for Research Excellence (TARE) (No-TAR/2018/000473 dtd 01-3-

2019). ARC thanks the X-ray facility of the Department of Chemical Sciences, IISER Mohali for single crystal X-ray diffraction data collection.

References

[1] Biomimetic Oxidations Catalyzed by Transition Metal Complexes, B. Meunier (Ed.), Imperial College Press, London, 2000.

[2] A. -F. Miller, FEBS Lett. 586 (2012) 585–595.

[3] Cytochrome P-450. Structure, Mechanism and Biochemistry, 2nd ed.; J. T. Groves, Y. Z. Han, P. R. Ortiz de Montellano, Eds. Plenum Press: New York, (1995) 3–48.

[4] W. Nam, Acc. Chem. Res. 40 (2007) 465.

[5] M. Costas, M. P. Mehn, M. P. Jensen, L. Que, Chem. Rev. 104 (2004) 939–986.

[6] (a) J. P. Layfield, S. Hammes-Schiffer, Chem. Rev. 114 (2014) 3466–3494; (b) M. Garai, D. Dey, H. R. Yadav, A. R. Choudhury, N. Kole, B. Biswas, Polyhedron, 129 (2017) 114-122; (c) D. Dey, M. Garai, S. Arar, A. Almherat, A. Al-Hunaiti, H. R. Yadav, M. Maji, A. R. Choudhury, B. Biswas, J. Mol. Struct. 1180 (2019) 220-226.

[7] (a) J. J. A. Cotruvo, J. Stubbe, Metallomics, 4 (2012) 1020–1036; (b) A. De, M. Garai, H. R. Yadav, A. R. Choudhury, B. Biswas, Appl. Organometal. Chem., 31 (2017) e3551.

[8] (a) D. Dey, A. De, H. R. Yadav, P. S. Guin, A. R. Choudhury, N. Kole, B. Biswas, ChemistrySelect 01 (2016) 1910-1916; (b) A. De, D. Dey, C. K. Pal, S. Paul, B. Biswas, J. Mol. Struct. 1195 (2019) 293-301.

[9] B. Das, A. Al-Hunaiti, M. Haukka, S. Demeshko, S. Meyer, A. A. Shteinman, F. Meyer, T. Repo, E. Nordlander. Euro. J. Inorg. Chem, 21 (2015) 3590-3601.

[10] (a) H. G. Jang, D. D. Cox, L. Que Jr, J. Am. Chem. Soc. 113 (1991) 9200-9204 ; (b) B. Chowdhury, M. Karar, S. Paul, M. Joshi, A. R. Choudhury, B. Biswas, Sens. Actuators, B 276 (2018) 560-566.

[11] M. Merkel, M. Pascaly, B. Krebs, J. Astner, S. P. Foxon, S. Schindler, Inorg. Chem. 44 (2005) 7582–7589.

[12] R. Rahaman, B. Chakraborty, T. K. Paine, Angew. Chem. Int. Ed. 55 (2016) 13838–13842.

[13] M. Bordeaux, A. Galarneau, J. Drone, Angew. Chem. Int. Ed. 51 (2012) 10712–10723.

[14] A. Al-hunaiti, M. Räisänen, T. Repo, Chem. Commun. 52 (2016) 2043-2046.

[15] (a) P. C. A. Bruijnincx, M. Lutz, A. L. Spek, W. R. Hagen, B. M. Weckhuysen, G. van Koten, R. J. M. K. Gebbink, J. Am. Chem. Soc. 129 (2007) 2275–2286; (b) D. Dey, S. Das, H. R. Yadav, A. Ranjani, L. Gyathri, S. Roy, P. S. Guin, D. Dhanasekaran, A. R. Choudhury, M. A. Akbarsha, B. Biswas, Polyhedron 106 (2016) 106-114.

[16] M. P. Valley, C. K. Brown, D. L. Burk, M. W. Vetting, D. H. Ohlendorf, J. D. Lipscomb, Biochemistry, 44 (2005) 11024–11039.

[17] A. K. Gupta, A. Dhir, C. P. Pradeep, Inorg. Chem. 55 (2016) 7492−7500.

[18] D. Dey, G. Kaur, A. Ranjani, L. Gyathri, P. Chakraborty, J. Adhikary, J. Pasan, D. Dhanasekaran, A. R. Choudhury, M. A. Akbarsha, N. Kole, B. Biswas, Eur. J. Inorg. Chem. 2014 (2014) 3350-3358;

[19] M. Karar, S. Paul, B. Biswas, P. Paul, T. Majumdar, A. Mallick , ChemistrySelect, 4 (2019) 10149-10156

[20] S. Das, A. Sahu, M. Joshi, S. Paul, M. Shit, A. R. Choudhury, B. Biswas, ChemistrySelect, 3 (2018) 10774-10781.

[21] R. Mayilmurugan, M. Sankaralingam, E. Suresh. Palaniandavar, Dalton Trans. 39 (2010) 9610–9625.

[22] M. Garai, A. Das, M. Joshi, S. Paul, M. Shit, A. R. Choudhury, B. Biswas, Polyhedron, 156 (2018) 223-230

[23] Y. Sakai, Y. Sagara, H. Nomura, N. Nakamura, Y. Suzuki, H. Miyazaki, C. Adachi, **Chem. Commun. 51** (2015) 3181-3184.

[24] M. Srinivas, G. R.Vijayakumar, K. M. Mahadevan, H. Nagabhushana, H. S. Bhojya Naik, Journal of Science: Advanced Materials and Devices, 2 (2017) 156-164

[25] M. -T. Chen, Y. -Y. Chen, G. -L. Li, C. -T. Chen, Front. Chem. 6 (2019) Art 615.

[26] A. Krezel, W. Maret, Archives of Biochemistry and Biophysics, 611 (2016) 3e19.

[27] K. A. McCall, C. -C. Huang, C. A. Fierke, J. Nutr. 130 (2000) 1437S-1446S.

[28] (a) V. A. Soldatenkov, M. Smulson, Int. J. Cancer 90 (2000) 59-67; (b) A. Castello, M. W. Hentze, T. Preiss, Trends Endocrinolmetals, 26 (2015) 746–757; (c) E. C. Friedberg,

G. C. Walker, W. Siede, R. D. Wood, R. A. Schultz, T. E. Berger, DNA repair & mutagenesis, 2nd Edn, ASM press, Washington, USA, 2006.

[29] Y. Zheng, C. Duanmu, Y. Gao, Org. Lett., 8 (2006) 3215–3217.

[30] (a) S. Uhlenbrock, R. Wegner, B. Krebs J. Chem. Soc., Dalton Trans., (1996) 3731-3736; (b) R. Bagai, K. A. Abboud, G. Christou, Dalton Trans. (2006) 3306–3312; (c) P. E. Kruger, B. Moubaraki, G. D. Fallon, K. S. Murray, J. Chem. Soc., Dalton Trans. (2000) 713–718.

[31] (a) B. Biswas, M. Mitra, J. Adhikary, G. R. Krishna, P. P. Bag, C. M. Reddy, N. Aliaga-Alcalde, T. Chattopadhyay, D. Das R. Ghosh, Polyhedron, 53 (2013) 264-268; (b) D. Dey, G. Kaur, M. Patra, A. R. Choudhury, N. Kole, B. Biswas, Inorg. Chim. Acta, 421 (2014) 335-341; (c) D. Dey, S. Pal, P. P. Bag, S. Saha, S. Chandraleka, D. Dhanasekaran, N. Kole, B. Biswas, J. Indian Chem. Soc. 92 (2015) 191-202; (d) B. Biswas, J. Indian Chem. Soc. 94 (2017) 811-818; (e) M. Karar, S. Paul, B. Biswas, T. Majumdar and A. Mallick, Dalton Trans. 47 (2018) 7059-7069.

[32] S. Pal, B. Chowdhury, M. Patra, M. Maji, B. Biswas, Spectrochim. Acta A, 144 (2015) 148–154.

[33] G. M. Sheldrick, SHELXT - Integrated space-group and crystal-structure determination Acta Cryst. A 71 (2015) 3-8.

[34] O. V. Dolomanov, L. J. Bourhis, R. J. Gildea, J. A. K. Howard, H. Puschmann, J. Appl. Cryst. 42 (2009) 339.

[35] L. J. Farrugia. J. Appl. Cryst. 45 (2012) 849.

[36] M. J. Turner, J. J. McKinnon, S. K. Wolff, D. J. Grimwood, P. R. Spackman, D. Jayatilaka, M. A. Spackman, Crystal Explorer, 17 (2017).

[37] M. A. Spackman, D. Jayatilaka, CrystEngComm. 11 (2009) 19-32.

[38] M. A. Spackman, J. J. McKinnon, CrystEngComm. 4 (2002) 378-392.

[39] C. K. Pal, S. Mahato, H. R. Yadav, A. R. Choudhury, B. Biswas, Polyhedron, 174 (2019) 114156.

[40] P. K. Mudi, R. K. Mahato, M. Joshi, S. Paul, A. R. Choudhury, B. Biswas, J. Mol. Struct. 1200 (2020) 127083.

[41] M. J. Frisch, G. W. Trucks, H. B. Schlegel, G. E. Scuseria, M. A. Robb, J. R. Cheeseman, G. Scalmani, V. Barone, B. Mennucci, G. A. Petersson, H. Nakatsuji, M. Caricato, X. Li, H. P. Hratchian, A. F. Izmaylov, J. Bloino, G. Zheng, J. L. Sonnenberg, M. Hada, M. Ehara, K. Toyota, R. Fukuda, J. Hasegawa, M. Ishida, T. Nakajima, Y. Honda, O. Kitao, H. Nakai, T. Vreven, J. A. Montgomery Jr, J. E. Peralta, F. Ogliaro, M. Bearpark, J. J. Heyd, E. Brothers, K. N. Kudin, V. N. Staroverov, R. Kobayashi, J. Normand, K. Raghavachari, A. Rendell, J. C. Burant, S. S. Iyengar, J. Tomasi, M. Cossi, N. Rega, J. M. Millam, M. Klene, J. E. Knox, J. B. Cross, V. Bakken, C. Adamo, J. Jaramillo, R. Gomperts, R. E. Stratmann, O. Yazyev, A. J. Austin, R. Cammi, C. Pomelli, J. W. Ochterski, R. L. Martin, K. Morokuma, V. G. Zakrzewski, G. A. Voth, P. Salvador, J. J. Dannenberg, S. Dapprich, A. D. Daniels, O. Farkas, J. B. Foresman, J. V. Ortiz, J. Cioslowski, D. J. Fox, Gaussian 09 (Revision A.02), Gaussian Inc., Wallingford, CT, 2009.

[42] T. H. Dunning and P. J. Hay, in Modern Theoretical Chemistry, ed. H. F. Schaefer, Plenum, New York, 3rd edn, 1976.

[43] (a) B. Mennucci, E. Cances, J. Tomasi, J. Phys. Chem. B. 101 (1997) 10506-10517;

(b) E. Cances, B. Mennucci, J. Tomasi, J. Chem. Phys. 107 (1997) 3032-3041;

(c) R. Cammi, J. Tomasi, J. Comput. Chem. 16 (1995) 1449-1458;

(d) S. Miertus, E. Scrocco, J. Tomasi, Chem. Phys. 55 (1981) 117-129.

[44] (a) S. Paul, M. Karar, B. Das, A. Mallick, T. Majumdar, Chem. Phys. Lett. 689 (2017) 199-205; (b) S. Paul, M. Karar, S. Mitra, S. A. S. Shah, T. Majumdar, A. Mallick, ChemistrySelect 1 (2016) 5547-5553; (c) A. De, A. Sahu, S. Paul, M. Joshi, A. R. Choudhury, B. Biswas, J. Mol. Struct. 1167 (2018) 187-193; (d) S. Paul, A. Mallick, T. Majumdar, Chem. Phys. Lett. 634 (2015) 29–36; (e) N. Dutta, S. Haldar, G. Vijaykumar, S. Paul, A. P. Chattopadhyay, L. Carrella, M. Bera, Inorg. Chem. 57 (2018) 10802-10820.

[45] M. N. Ahamad, M. Kumar, A. Ansari, I. Mantasha, M. Ahmad, M. Shahid, New J. Chem. 43 (2019) 14074-14083.

[46] S. Anbu, S. Kamalraj, B. Varghese, J. Muthumary, M. Kandaswamy, Inorg. Chem. 51 (2012) 5580−5592.

[47] H. Arora, S. K. Barman, F. Lloret, R. N. Mukherjee, Inorg. Chem. 51 (2012) 5539−5553.

[48] R. Bonomi, F. Selvestrel, V. Lombardo, C. Sissi, S. Polizzi, F. Mancin, U. Tonellato, P. Scrimin, J. Am. Chem. Soc. 130 (2008) 15744−15745.

[49] C. Vichard, T. A. Kaden, Inorg. Chim. Acta, 337 (2002) 173−180.

[50] J. Chen, X. Wang, Y. Zhu, J. Lin, X. Yang, Y. Li, Y. Lu, Z. Guo, Inorg. Chem. 44 (2005) 3422−3430.

[51] J. He, J. Sun, Z. -W. Maoa, L. -N. Ji, H. J. Sun, Inorg. Biochem. 103 (2009) 851−858.

[52] R. Sanyal, A. Guha, T. Ghosh, T. K. Mondal, E. Zangrando, D. Das, Inorg. Chem. 53 (2014) 85-96

[53] A. Erxleben, Front. Chem. 7 (2019) Art 82

[54] R. Sanyal, X. Zhang, P. Kundu, T. Chattopadhyay, C. Zhao, F. A. Mautner, D. Das, Inorg. Chem. 54 (2015) 2315−2324.

[55] X. Zhang, Y. Zhu, X. Zheng, D. L Phillips, C. Zhao,. Inorg. Chem. 53 (2014) 3354−3361.

[56] C. I. Maxwell, N. J. Mosey, R. S. Brown, J. Am. Chem. Soc. 135 (2013) 17209−17222.

[57] H. Daver, B. Das, E. Nordlander, F. Himo, Inorg. Chem. 55 (2016) 1872−1882.

Table 1. Crystallographic data and structure refinement parameters for Zn(II)-Schiff base complex.

Parameters	**Compound 1**
Empirical formula	$C_{17}H_{18}N_2O_5Zn$
Formula weight	379.70
T (K)	100
Wavelength (Å)	0.71073
Crystal system	Hexagonal
Space group	$P6_1$
Unit cell dimensions	
a (Å))	26.492(3)
b (Å)	26.492(3)
c (Å)	5.1701(8)
α (°)	90.0
β (°)	90.0
γ (°)	120.0
V ($Å^3$)	3142.4(7)
Z	6
ρ (gm cm^{-3})	1.204
Absorption coefficient (mm^{-1})	1.191
F(000)	1176
Crystal size (mm^3)	0.1×0.1×0.11
Index ranges (h, k, l)	-38,28; -33,40; -7, 7
Reflections collected	23830
Independent reflections	14147
R(int)	0.077
Final R indices [I>2sigma(I)]	R1 = 0.0695, wR2 = 0.1681
Largest diff. peak and hole	1.49 and -0.46 e.$Å^{-3}$

Table 2. Selected bond distances (Å) and bond angles (°) for Zn(II) complex.

Bond length (Å)					
	XRD	DFT		XRD	DFT
Zn1-O1	2.025(5)	2.012	Zn1-N2	2.142(7)	2.060
Zn1-O2	2.017(5)	1.956	Zn1-N1	2.093(9)	2.060
Zn1-O3	1.983(5)	2.182			
Bond angles (°)					
	XRD	DFT		XRD	DFT
O2-Zn1-O3	106.2(2)	96.1	O3-Zn1-N2	100.2(3)	94.3
O1-Zn1-O2	81.80(2)	110.3	O3-Zn1-N1	106.5(3)	136.1
O1-Zn1-N1	88.1(3)	88.1	O1-Zn1-N2	159.0(3)	156.1
O2-Zn1-N1	147.0(3)	127.7	O1-Zn1-N1	88.1(3)	88.1
O1-Zn1-O3	100.2 (2)	72.27	N1-Zn1-N2	91.2(3)	88.6

Table 3. Kinetic parameters for transesterification activity by Zn(II)-Schiff base complex in aqueous methanol medium.

Complex	**Substrate**	**Medium**	k_{cat} **(s^{-1})**	Reference
$[Zn(H\mathbf{L})(H_2O)].(H_2O)$*	NPP	methanol-water	7.55×10^{-2}	Present
$[Zn_2\mathbf{L}]$	NPP	acetonitrile-water,	476−203	46
$[Zn_2(\mathbf{L}^2)(\mu\text{-}OAc)_2(MeCN)_2][PF_6]$	HPNP	methanol-water	3.44×10^{-4}	47
$[MPGN\text{-}Zn^{II}]$	BNPP	water-methanol	3.60×10^{-5}	48
$[Zn_2(LH_{-2})]^{2+}$	BNPP	water	2.26×10^{-6}	49
$[Zn_2(L_{2H})(AcO)(H_2O)](PF_6)]0.2H_2O$	BNPP	methanol-water	4.60×10^{-6}	50
$[Zn(bpy)Cl_2]$	BNPP	water	5.74×10^{-7}	51
$[Zn(HL^2)X_2]$	NPP	$DMF\text{-}H_2O$	2-10	52

*V_{max} (M s^{-1}) = 7.55×10^{-6} (Std. Error 2.21×10^{-7}); K_m (M) = 2.27×10^{-3} (Std. Error 5.38×10^{-4})

Where NPP =Nitro phenyl phosphate; BNPP = Bis(4-nitrophenyl)phosphate.; HPNP = 2-Hydroxypropyl(4-nitrophenyl)-phosphate

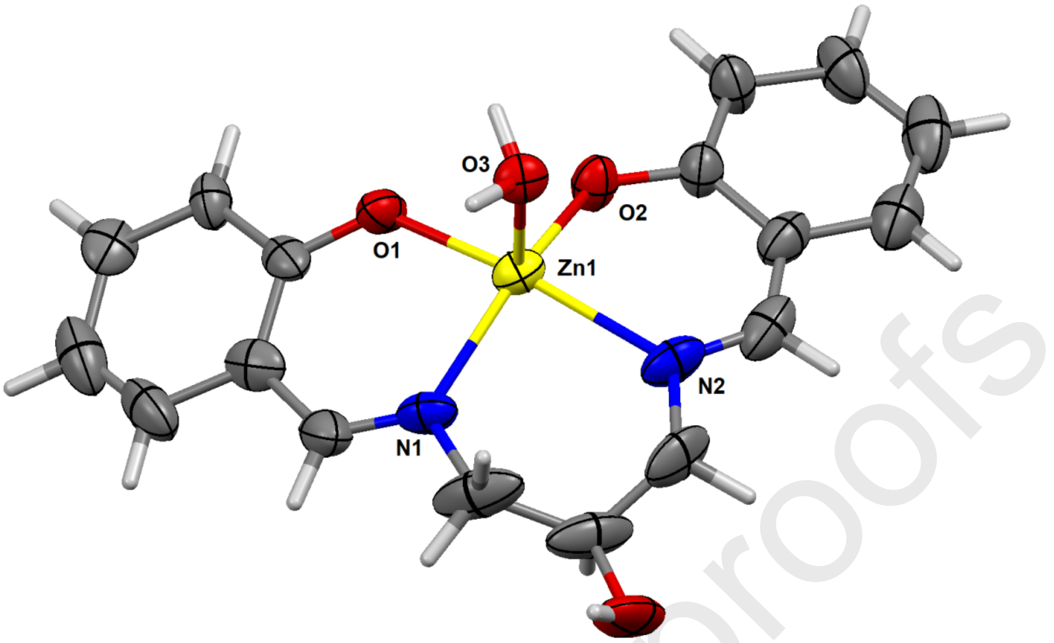

Fig 1. ORTEP diagram of Zn(II)-Schiff base complex (**1**) with 30% ellipsoid probability.

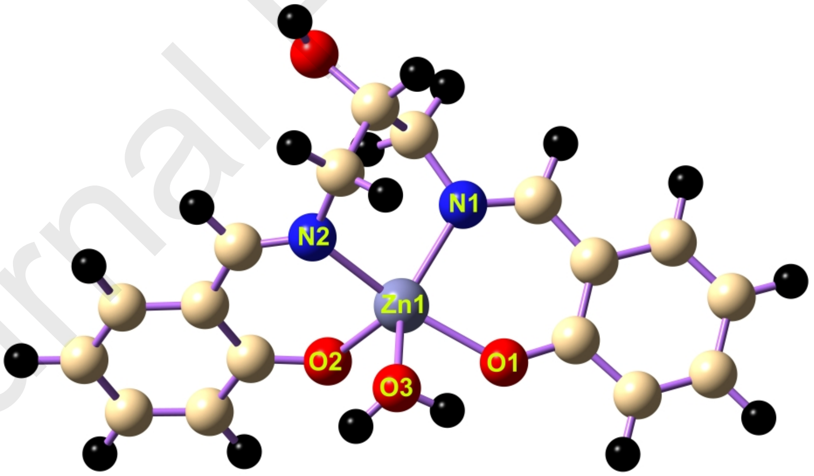

Fig 2. Optimized structure of Zn(II) complex in vacuum obtained using B3LYP/6-311G theoretical model.

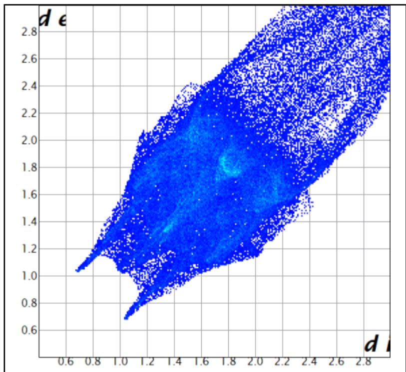

All in – All out

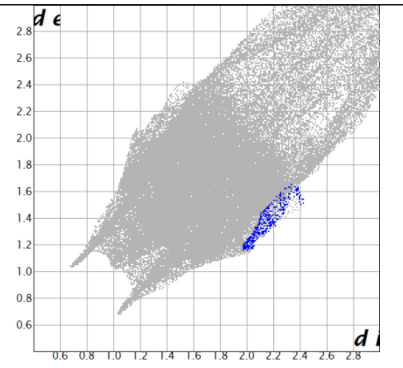

Zn in – All out

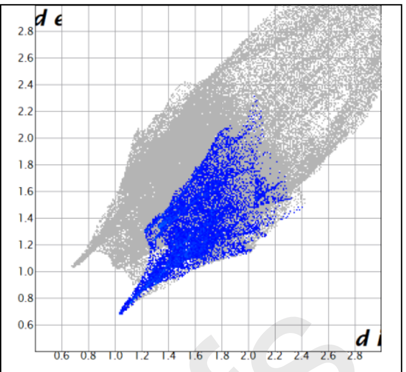

O in – All out

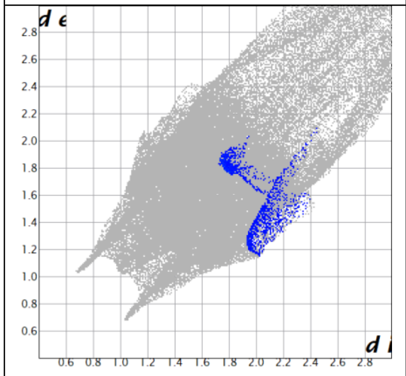

N in – All out

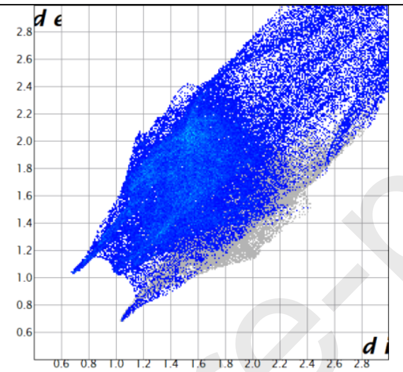

H in – All out

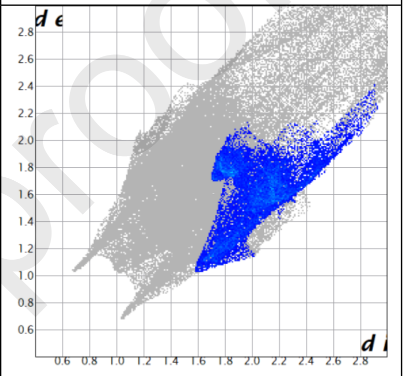

C in – All out

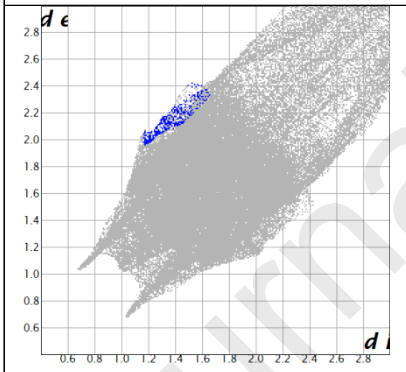

All in – Zn out

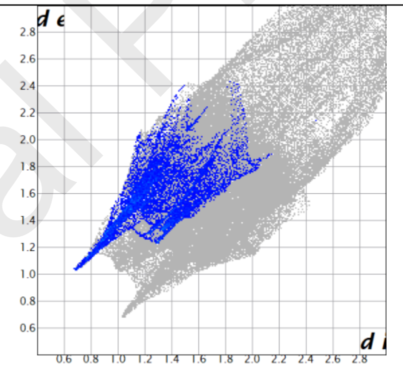

All in – O out

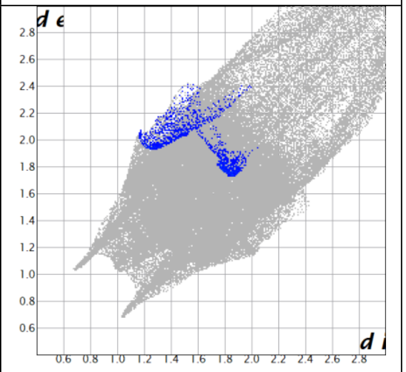

All in – N out

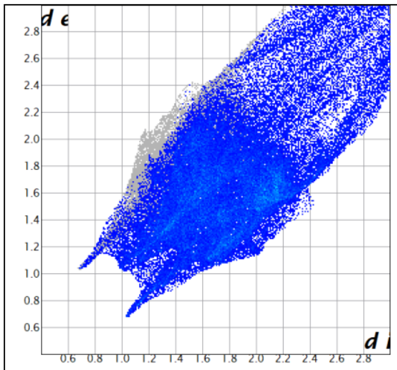	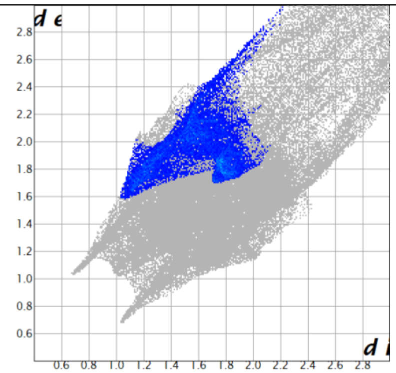	
All in – H out	**All in – C out**	

Fig 3. Fingerprint plot of Zn(II)-Schiff base complex

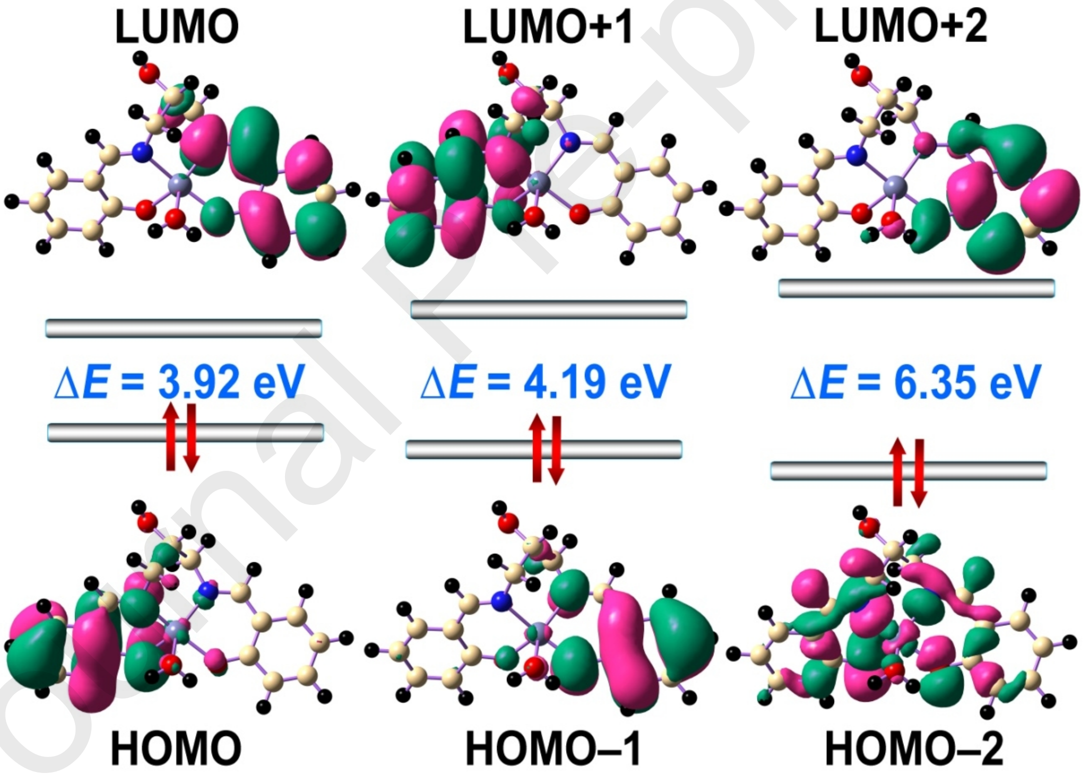

Fig. 4. Images of frontier molecular orbital of Zn(II) complex in IEFPCM/MeOH solvent system.

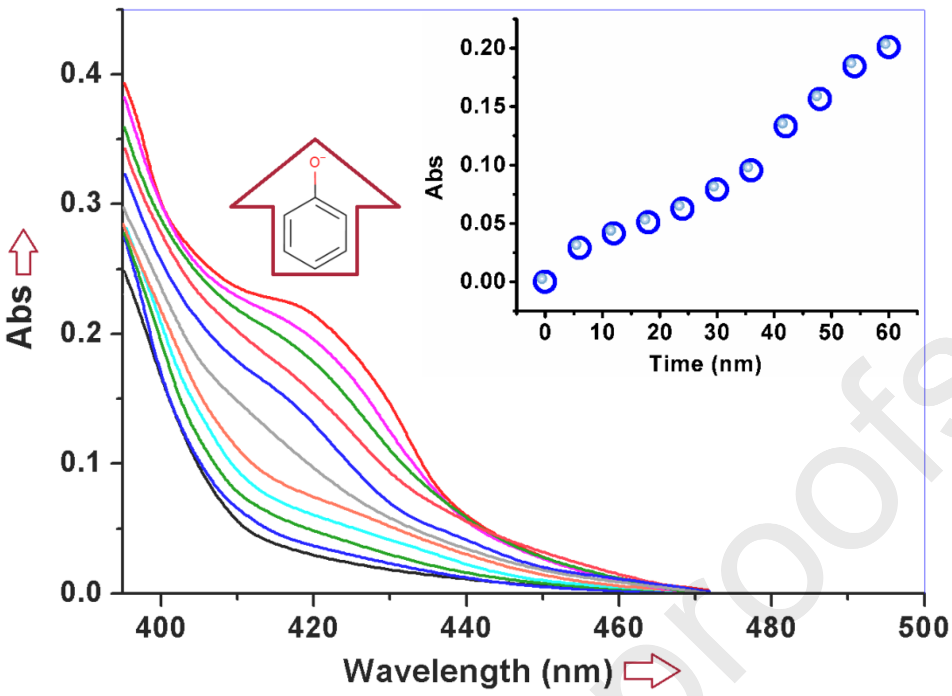

Fig 5. Increase of 4-nitrophenolate band at 418 nm after addition of zinc(II)-Schiff base complex to 100 equivalents of PNPP in aq. methanolic solution. (The spectra were recorded after every 06 min). Inset: Absorbance vs Time plot at defined wavelength.

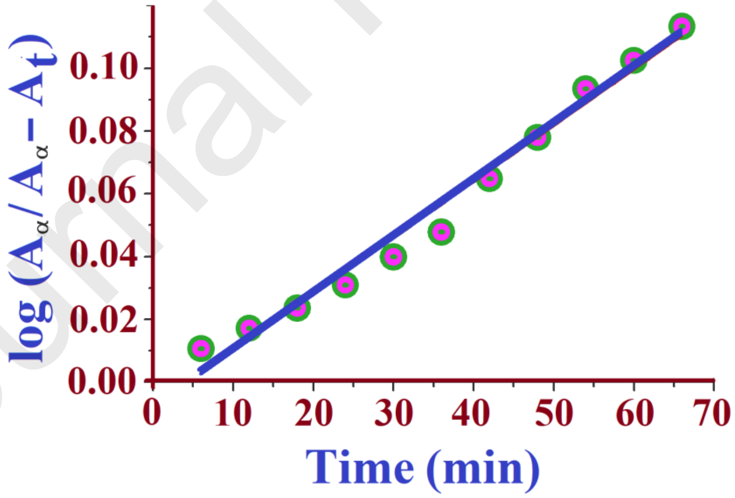

Fig 6. Initial rate determination for phosphoester cleavage activity by Zn(II)-Schiff base complex towards PNPP using plot of time vs $\log[A_\alpha/(A_\alpha\text{-}A_t)]$ of the same solution.

Transesterification Activity by a Zinc(II)-Schiff Base Complex with Theoretical Interpretation

Chanchal Kumar Pal,[a] Shreya Mahato,[a] Mayank Joshi,[b] Suvendu Paul,[c] Angshuman Roy Choudhury, [b] Bhaskar Biswas[a,*]

[a]*Department of Chemistry, University of North Bengal, Darjeeling-734013, India*
[b]*Department of Chemical Sciences, Indian Institute of Science Education and Research, Mohali, Sector 81, Knowledge City, S. A. S. Nagar, Manauli PO, Mohali, Punjab 140306, India*

[c]*Department of Chemistry, University of Kalyani, Kalyani 741235, West Bengal, India*

The present study accounts on the synthesis, structural characterization, self-assembled crystalline architecture, and transesterification study of a mononuclear zinc(II) complex, [Zn(H**L**)(H_2O)].(H_2O) (**1**) containing a previously reported Schiff base ligand, H_3**L** = *N,N′*-bis(salicylidene)-1,3-diamino-2-propanol].

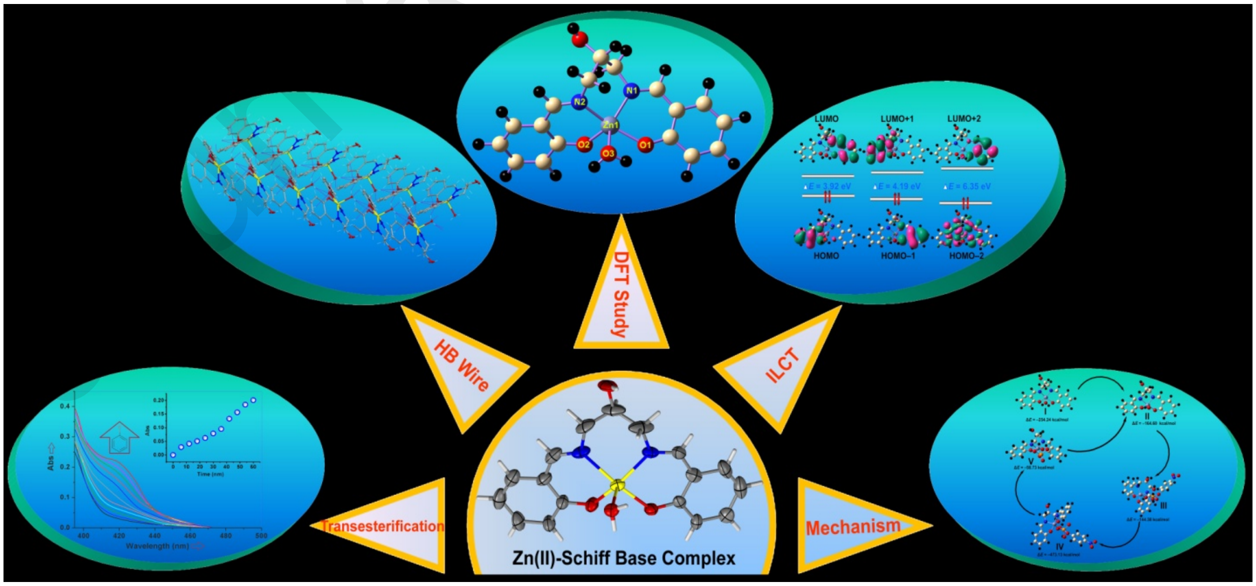

Highlights

- Synthesis and characterization of a tetrapyramidal zinc(II)-Schiff base complex
- Zn(II) complex crystallizes in hexagonal crystal system with $P6_1$ space group.
- This Zn(II)-Schiff base complex displays good transesterification activity with initial rate constant, V(min^{-1}) = 1.73×10^{-4}
- Computational studies agree well with the experimental results in this course of study.

Chanchal Kumar Pal: Conceptualization, Curation, Formal analysis, Methodology, Investigation; **Shreya Mahato**: Formal analysis, Investigation, Draft manuscript preparation, **Mayank Joshi**: Visualization; **Suvendu Paul:** Software; **Angshuman Roy Choudhury**: Validation; **Bhaskar Biswas**: Writing-Reviewing and Editing, Supervision.

Conflict of Interest and Authorship Conformation Form

Please check the following as appropriate:

- ○ All authors have participated in (a) conception and design, or analysis and interpretation of the data; (b) drafting the article or revising it critically for important intellectual content; and (c) approval of the final version.

- ○ This manuscript has not been submitted to, nor is under review at, another journal or other publishing venue.

- ○ The authors have no affiliation with any organization with a direct or indirect financial interest in the subject matter discussed in the manuscript

- ○ The following authors have affiliations with organizations with direct or indirect financial interest in the subject matter discussed in the manuscript:

Author's name	Affiliation
Chanchal Kumar Pal	*University of North Bengal, Darjeeling-734013*

Shreya Mahato	*University of North Bengal, Darjeeling-734013*
Bhaskar Biswas	*University of North Bengal, Darjeeling-734013*
Mayank Joshi	*Indian Institute of Science Education and Research, Mohali*
Angshuman Roy Choudhury	*Indian Institute of Science Education and Research, Mohali*
Suvendu Paul	*Department of Chemistry, University of Kalyani, Kalyani 741235,India*